I&EC research
Industrial & Engineering Chemistry Research

Article

pubs.acs.org/IECR

Economic Plantwide Control of the Cumene Process

Vivek Gera,[†] Mehdi Panahi,[‡] Sigurd Skogestad,[‡] and Nitin Kaistha*[,†,§]

[†]Chemical Engineering, Indian Institute of Technology Kanpur, Kanpur, 208016, India

[‡]Chemical Engineering, Norwegian University of Science and Technology, Trondheim, Norway

ABSTRACT: Economic plantwide control of the cumene process over a large throughput range (design to maximum achievable throughput) is studied. The process has 12 steady state operating degrees of freedom (DOFs), which are optimized for maximum hourly profit. At maximum throughput, the highest number of constraints (eight) is active leaving four unconstrained degrees of freedom. Reasonable controlled variables (CVs) corresponding to these are chosen with implementation of a constant setpoint policy at lower throughputs providing near optimal operation. For economic plantwide control, the best pairings for tight control of the maximum throughput active constraints and self-optimizing CVs are first implemented followed by inventory control loop pairings using the remaining valves. The resulting control structure consists of long level loops that manipulate the two fresh feeds to maintain the bottom sump level of the first two distillation columns. Simulation results show that the unconventional control structure provides smooth operation over the wide throughput range with tight control of the active constraints and the self-optimizing CVs. Comparison with a conventional plantwide control system (throughput manipulator at fresh propylene feed) shows that the synthesized control structure is simpler in requiring no overrides for handling constraints and achieving superior economic performance.

INTRODUCTION

Plantwide control system design for safe, stable, and economic (efficient) operation of integrated chemical processes has been actively researched for over two decades now. The plantwide control problem is particularly challenging due to the combinatorial complexity in the possible input−output pairing choices for controlling regulatory, economic, and safety related control objectives with several possible workable control structures for a given process. In seminal early work, Luyben and co-workers highlighted key plantwide regulatory control issues such as the snowball effect[1] in reactor−separator−recycle systems and suggested control system structuring guidelines for addressing the same.[2] The many case studies on plantwide control structure design[3−5] lead to a systematic nine-step plantwide control design procedure.[6] The procedure accounts for the control degrees of freedom and control objectives (steps 1 and 2), chooses the throughput manipulator (step 3), then goes on to pair loops in a hierarchy of first controlling potential instabilities (reactor thermal runaway) (step 4) followed by economic (e.g., product quality), safety, and environmental objectives (step 5), and finally performs consistent inventory management (steps 6 and 7). Any remaining control valves are used for local unit controls (step 8) and further improvement of dynamic controllability/economic control (step 9). The crucial step of formulating the control objectives is based on engineering judgment and heuristics.

To systematize the formulation of the control objectives, Skogestad[7] proposed using steady state optimization of an economic objective function to obtain the optimally active constraints and self-optimizing variables corresponding to any unconstrained steady state degrees of freedom (DOFs). By definition, for an appropriate constant value of a self-optimizing variable, the steady state economic loss (from optimum) is insensitive to disturbances. The plantwide control system design problem then boils down to implementing loops for controlling the active constraints, the self-optimizing variables (SOV), and the process inventories (levels, pressures, component inventories, etc.). Skogestad[8] proposed using a bottom-up approach for loop pairing; the inventory control loop pairings being selected first in the regulatory layer followed by a supervisory layer of economic loops (active constraints and self-optimizing variables) that adjust setpoints in the regulatory layer. Recent literature reports[9−13] show that the alternative top-down pairing approach, where economic pairings are first selected followed by the regulatory pairings, achieves significant reduction in the back-off in dominant active constraint(s) for superior economic performance along with acceptable regulatory control.

Regardless of the loop pairing approach (top-down or bottom-up), much of the plantwide control literature addresses control system design for process operation around the design throughput, where process equipment are away from any capacity constraints (due to equipment overdesign), that is, for unconstrained process operation. In practice, depending on the prevailing business scenario, a plant must be operated significantly above or below the design throughput for sustained periods, possibly including process operation at maximum throughput. As throughput is increased, equipment sequentially hit (hard) capacity constraints and crucial control tasks such as product quality control or inventory stabilization may be lost. The active constraint set then expands, and the SOV set contracts due to the loss in DOFs.

Conventionally, such additional constraints are handled by providing appropriate override controllers that alter the material balance control structure from the (hard) constrained unit operation until the process feed. To avoid such cumbersome

Received: May 28, 2012
Revised: November 15, 2012
Accepted: December 9, 2012

   dx.doi.org/10.1021/ie301386h | *Ind. Eng. Chem. Res.* XXXX, XXX, XXX−XXX

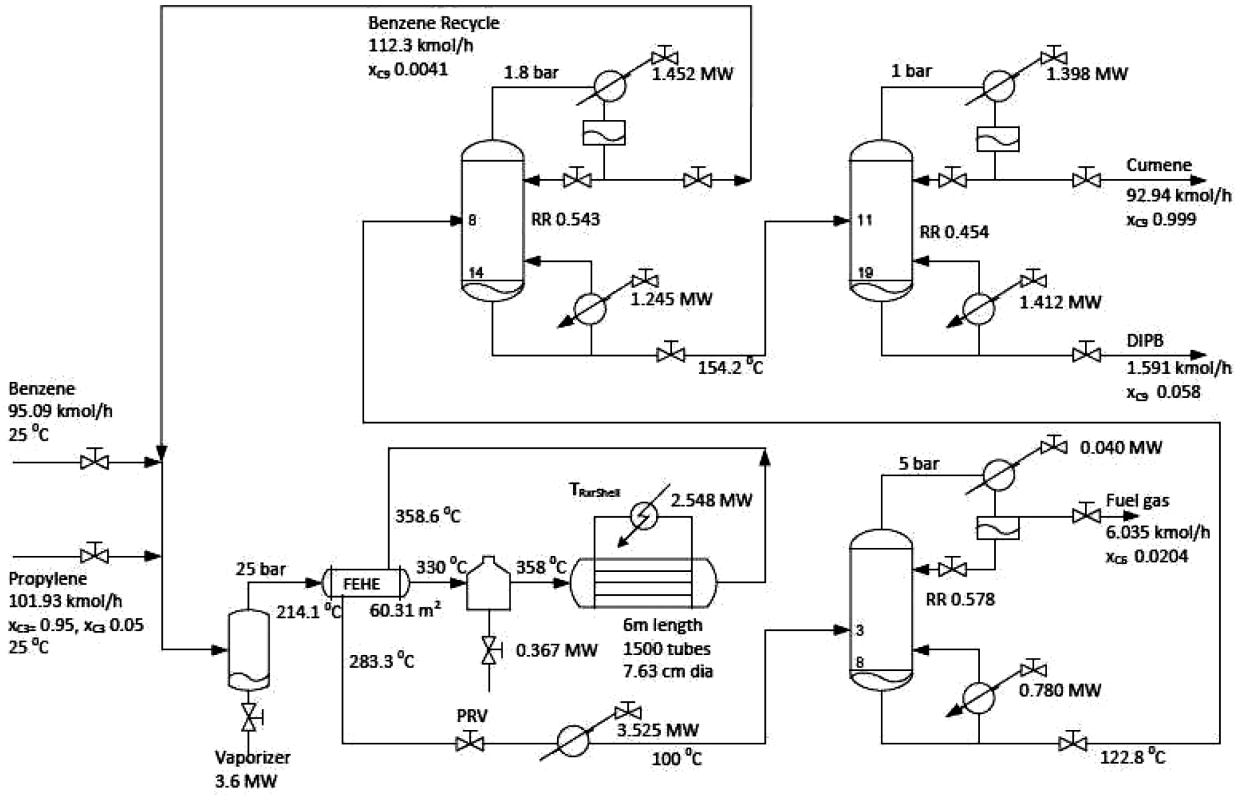

Figure 1. Cumene process schematic with salient design and base-case operating parameters.

overrides and simplify the overall plantwide control system, through a series of recent case studies,[9−11] Kaistha and co-workers have propounded developing a robust control system for process operation at maximum throughput, where the highest number of constraints are active, and then adapting it for taking up SOV control at lower throughputs, where additional setpoints become available for manipulation due to constraints becoming inactive. Jagtap et al.[14] have proposed a systematic five-step procedure for top-down synthesis of such an economic plantwide control system that gives (near) optimal process operation over a wide throughput range.

In this work, we demonstrate the application of this procedure to the cumene process, recently studied by Luyben.[15] The main contribution of the work is in demonstrating that the top-down approach to plantwide control system design results in an unconventional plantwide control system providing acceptable regulatory control (stabilization) with significant economic benefit due to tight economic variable control. Further, the additional complexity of override controllers that alter the material balance structure for constraint handling is avoided.

In the following, the process is briefly described followed by steady state optimization results over a wide throughput range including maximum throughput. The economic plantwide control structure is then synthesized. For comparison, a conventional plantwide control structure with fresh propylene (limiting reactant) feed as the throughput manipulator is also synthesized. The two control structures are then dynamically evaluated and compared for a transition from design throughput to maximum throughput as well as for constrained/unconstrained process operation for various disturbance scenarios. The salient findings conclude the article.

PROCESS DESCRIPTION

Figure 1 provides a schematic of the cumene process along with the design and base-case salient operating conditions. Fresh benzene (C_6) and fresh propylene (95 mol % propylene and 5 mol % propane), mixed with recycle benzene, are vaporized in a vaporizer. The vapor stream is preheated using the hot reactor effluent in a feed effluent heat exchanger (FEHE) before being heated to the reaction temperature in a furnace. The heated stream is fed into a packed bed reactor (PBR), a shell and tube heat exchanger with catalyst loaded tubes, and pressurized coolant on the shell side. Propylene (C_3) and C_6 react in the vapor phase to produce cumene (C_9), which can further react with C_3 to produce a small amount of di-isopropyl benzene (C_{12} or DIPB) side product. The reactor effluent loses sensible heat in the FEHE and is partially condensed in a cooler. The cooled stream with C_9, C_{12}, unreacted reactants, and inert propane is fed to a three column light-out-first distillation train. The purge column recovers inert propane and any unreacted propylene with some benzene as vapor distillate (used as fuel gas). The bottoms is sent to the recycle column which recovers the unreacted benzene as the distillate and recycles it. The recycle column bottoms is sent to the product column, which recovers nearly pure C_9 distillate product and heavy C_{12} (plus some C_9) bottoms. The process thus discharges C_{12}, which is used as a fuel.

The reaction chemistry and kinetics used to model the process are taken from the work of Luyben.[15] The NRTL physical property method is used to model thermodynamic properties. Steady state simulation was performed using UniSim Design R390 version 3.61.0.0 from Honeywell. The flowsheet studied here differs from Luyben's flowsheet in that the first distillation column replaces a flash tank to mitigate loss of precious benzene in the C_3 fuel gas stream. The optimized base-case process design and steady state operating conditions are also shown in Figure 1.

dx.doi.org/10.1021/ie301386h | Ind. Eng. Chem. Res. XXXX, XXX, XXX−XXX

This revised design gives 6.8% higher profit[16] than Luyben's flowsheet. This is primarily due to reduction in loss of precious benzene in the fuel gas stream from 3.96 to 0.13 kmol/h by replacement of the flash drum with a distillation column. The fresh benzene feed for the same propylene processing rate is then lower in the revised flowsheet. The extra revenue due to reduced benzene consumption is substantially higher than the slight increase in the capital and energy cost (a detailed economic comparison is provided in the Appendix).

OPTIMAL STEADY STATE PROCESS OPERATION

Degrees of Freedom. There are 22 independent control valves for the process as shown in Figure 1. Of these, seven valves will get used for regulating seven surge drum levels, namely, reflux drum and sump levels on each of the three columns (two levels/column × three columns = six levels) and the reactor feed vaporizer level. Also, three valves will get used to maintain the pressure of each of the three columns at the design value. This leaves $22 - 7 - 3 = 12$ free control valves that may be adjusted for process operation at the desired (hopefully optimum) steady state. The steady state operating DOFs for the process is then 12. Specification variables corresponding to these degrees of freedom chosen for robust flowsheet convergence are the following: fresh propylene feed (F_{C3}), total benzene flow (F_{C6Tot}), reactor inlet temperature (T_{rxr}), reactor coolant temperature ($T_{RxrShell}$), reactor pressure (P_{Rxr}), reactor effluent cooler outlet temperature (T_{cooler}), first column vent temperature, and bottoms propane mole fraction (T_{vent}^{D1} and x_{C3}^{B1}), the recycle column distillate cumene and the bottoms benzene mole fractions (x_{C9}^{D2} and x_{C6}^{B2}), and, finally, the product column distillate cumene and the bottoms cumene mole fractions (x_{C9}^{D3} and x_{C9}^{B3}). These 12 specification variables can be adjusted to achieve a given objective such as maximum throughput/profit or maximum yield/selectivity.

Steady State Economic Optimization. In this work, the steady state hourly operating profit, P, defined as

$$P = [\text{product revenue} - \text{raw material cost} - \text{energy cost}] \text{ per hour}$$

is used as a quantitative economic criterion that is maximized using the available steady state DOFs. The cost data is taken from the work of Gera et al.[16] We consider two modes of steady process operation. In mode I, the desired throughput (production rate or feed processing rate) is specified, usually based on business considerations. For processes with undesirable side products, such as the cumene process considered here, the optimization typically attempts to maximize the yield to desired product. For processes with no undesirable side products (e.g., a separation train), the optimization attempts to minimize the energy consumption per kilogram product. In mode II, the throughput itself is a decision variable for maximizing the economic criterion. Often, the mode II solution corresponds to steady process operation at/near the maximum achievable throughput.

For the cumene process considered here, in mode I, since the fresh propylene feed (F_{C3}) is fixed, only the remaining 11 DOFs need to be optimized. In mode II, all 12 DOFs (including F_{C3}) need to be optimized. The optimization is subject to physical and operational process constraints such as maximum/minimum material/energy flows, temperatures, pressures, product impurities, etc. These limits are obtained based on common engineering design practice for major equipment. Thus e.g., maximum liquid material flow limit is considered to be twice the design (base case) flow as the pumps are highly overdesigned. On the other hand, since distillation columns operate at ~80% flooding limit at base case, the maximum boilup limit is chosen as 1.25 × base-case boilup (approx.). The choice of the maximum reactor pressure is usually limited by the equipment thickness and typically the reaction section would be operated at the maximum allowable pressure for the highest reaction rate (and conversion) with no selectivity penalty. We have therefore taken the base-case design pressure (25 bar in Luyben's flowsheet) as the maximum reactor pressure.

Ideally all decision variables should be optimized simultaneously, but this can result in an unwieldy problem with poor convergence. The optimization is therefore simplified by applying engineering reasoning to optimize only the dominant decision variables affecting the economic criterion with reasonable values for the remaining decision variables. For the cumene process, the reactor effluent cooler temperature (T_{cooler}) has very little impact on the economic objective function (P) and is therefore kept fixed at 100 °C, a reasonable value that ensures the reactor effluent vapor is condensed. Similarly, the yearly operating profit is insensitive to changes around the base design values of the propane mol fraction leaking down the first column bottoms (x_{C3}^{B1}) and the cumene mole fraction leaking up the second column distillate (x_{C9}^{D2}). These are therefore kept fixed at the base values. Also, the first column vapor vent stream temperature (T_{vent}^{D1}) is set by the cooling water at 32 °C.

These simple engineering arguments fix four specifications simplifying the optimization to seven decision variables for mode I (given F_{C3}) and eight for mode II. The optimization is performed using Matlab's *fmincon* routine with Unisim as the background steady state flowsheet solver. The constrained optimization problem formulation (including price data and process constraints) and results for mode I and II are briefly summarized in Table 1.

The optimization results are interpreted as follows. The minimum product purity constraint ($x_{C9}^{D3MIN} = 99.9\%$) is active in both mode I and II, i.e. at all throughputs, for on-aim product quality with no product give-away. The maximum reactor operating pressure (P_{Rxr}^{MAX}) and maximum recycle (second) column boilup (V_2^{MAX}) constraints are active at all throughputs. Reactor operation at maximum operating pressure causes the reactor temperature to be lower for a given conversion improving selectivity (cumene product yield). Recycle column operation at maximum boilup causes the total (fresh + recycle) benzene to the reactor to be as high as possible, again enhancing selectivity with a higher reactor benzene to propylene ratio. As throughput is increased, the product column maximum boilup constraint, V_3^{MAX}, goes active. Even as the throughput may be further increased by, e.g., reducing the recycle column reflux (i.e., x_{C9}^{D2} is increased) and adjusting T_{Rxr} and $T_{RxrShell}$ to maintain conversion and selectivity, the Q_{fur}^{MIN} constraint goes active after which the selectivity decreases dramatically. The increase in throughput achieved is very marginal at <1 kmol/h. We therefore treat V_3^{MAX} going active as corresponding to the maximum economic throughput (mode II) with $F_{C3} = 169.96$ kmol/h. The significant increase (~70%) over the design throughput is a consequence of the extra processing capacity due to equipment overdesign as well as appropriate adjustment of steady state DOFs such as reactor inlet temperature and reactor coolant temperature as well as the C_6/C_{12} impurity mix in the cumene product and higher C_9 loss down the product column bottoms. Such large increases in throughput are usually realized for existing plants only after

dx.doi.org/10.1021/ie301386h | Ind. Eng. Chem. Res. XXXX, XXX, XXX−XXX

Table 1. Process Optimization Formulation and Results' Summary

objective	maximize (J)	
	J: hourly operating profit[a]	
process constraints	$0 \le$ material flows ≤ 2 (base case)	
	$0 \le V_1, V_2, V_3 \le 1.5$ (base case)	
	vent temperature = 32 °C	
	$0 \le$ energy flows ≤ 1.7 (base case)	
	1 bar $\le P_{Rxr} \le$ 25 bar	
	cumene product purity $\ge$ 0.999 mol fraction	
decision variable	mode I	mode II
F_{C3}	101.93 kmol/h_{Fixed}	169.96 kmol/h
F_{C6}^{Total}	294.16 kmol/h	316.2 kmol/h
T_{rxr}	322.26 °C	318.58 °C
$T_{RxrShell}$	368.95 °C	367.98 °C
P_{Rxr}	25 bar_{Max}	25 bar_{Max}
T_{cooler}	100 $°C_{Fixed}$	100 $°C_{Fixed}$
T_{vent}^{D1}	32 $°C_{Fixed}$	32 $°C_{Fixed}$
x_{C3}^{B1}	0.1%$_{Fixed}$	0.1%$_{Fixed}$
x_{C9}^{D2}	0.4%$_{Fixed}$	0.4%$_{Fixed}$
x_{C6}^{B2}	0.09%	0.05%
x_{C9}^{D3}	99.9%$_{Min}$	99.9%$_{Min}$
x_{C9}^{B3}	0.4%	10%
optimum J	\$3.809 × 10^3 h^{-1}	\$5.879 × 10^3 h^{-1}
F_{C9}	93.59 kmol/h	150.05 kmol/h
active constraints	x_{C9}^{D3MIN}, P_{Rxr}^{MAX}, V_2^{MAX}	x_{C9}^{D3MIN}, P_{Rxr}^{MAX}, V_2^{MAX}, V_3^{MAX}

[a]Heater duty \$16.8 1/GJ; steam \$9.83 1/GJ; cooling water \$0.16 1/GJ; F_{C6} \$68.5 1/kmol; F_{C3} \$34.3 1/kmol; F_{C9} \$150.0 1/kmol.

sufficient process operation experience and not immediately after commissioning.

It is instructive to compare the propylene conversion and yield-to-cumene (selectivity) for modes I and II. The propylene conversion reduces slightly from 98.6% in mode I to 98.1% in mode II. On the other hand, the selectivity shows a higher decrease from 98.25% in mode I to 95.15% in mode II. The decrease in selectivity is primarily attributed to the reduction in reactor feed benzene to propylene excess ratio as throughput is increased with the recycle benzene flow being nearly constant (fixed by V_2^{MAX}). The optimal mode I/II operation corresponds to ensuring near complete propylene conversion at as high a selectivity as possible, the latter being limited by the benzene recycle capacity of the second (recycle) column.

The three mode I active constraints (x_{C9}^{D3MIN}, P_{Rxr}^{MAX}, and V_2^{MAX}) along with the throughput specification (F_{C3}) leave four unconstrained DOFs. In mode II, the throughput is not specified and gets determined by the value of the additional V_3^{MAX} constraint so that the number of unconstrained DOFs remains four. The unconstrained optimum values of the four decision variables, x_{C9}^{B3}, x_{C6}^{B2}, T_{Rxr}, and $T_{RxrShell}$ are reported in Table 1 for modes I and II.

The low mode I optimum x_{C9}^{B3} reduces the loss of precious cumene down the product column bottoms without a prohibitively high energy cost. The optimum mode II x_{C9}^{B3} is much higher at 10%. This reduces the recycle column stripping load so that the V_3^{MAX} constraint goes active at higher throughputs for increased profit. Further loosening x_{C9}^{B3} however causes the profit to decrease due to excessive cumene loss in the side product stream.

The mode I optimum benzene leakage down the recycle column bottoms, x_{C6}^{B2}, is on the higher side at 0.09% so that benzene is the principal cumene product impurity. This is reasonable as benzene is the cheaper product impurity with DIPB consuming two extra moles of propylene. The mode II optimum x_{C6}^{B2} value reduces to 0.05% so that the two product impurities are comparable. As shown in Figure 2, this balances throughput and selectivity with V_2^{MAX} and V_3^{MAX} active constraints. If x_{C6}^{B2} is too high, the DIPB leakage in the product column distillate is prohibitively small requiring high reflux so that the V_3^{MAX} constraint goes active at a significantly lower throughput. Similarly, if x_{C6}^{B2} is too low, the feed that can be processed by

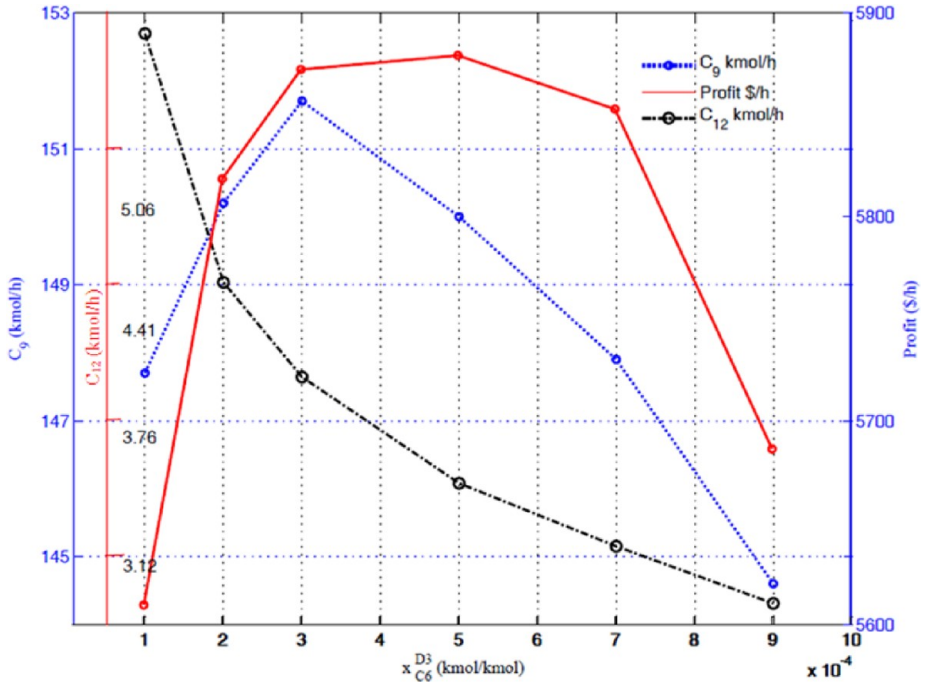

Figure 2. Optimum benzene impurity level in cumene product.

dx.doi.org/10.1021/ie301386h | Ind. Eng. Chem. Res. XXXX, XXX, XXX−XXX

the recycle column maintaining its two separation specifications without violating the V_2^{MAX} constraint is lower implying a loss in throughput. Also, as x_{C6}^{B2} is loosened, with V_2^{MAX} active, the benzene recycle increases for better selectivity with lower DIPB formation. Comparable amounts of the two principal impurities in the product balances these effects.

Optimal Operating Policy. We now seek a simple steady state operating policy that ensures near optimal operation over the entire throughput range. For economically optimal operation, we would like tight control of the active constraints and prudent management of the remaining unconstrained steady state DOFs using SOVs. Preferably, the CVs corresponding to the unconstrained steady state DOFs should be measurements that are cheap, reliable, fast, robust, and dynamically well behaved with respect to the manipulated variables (MVs). These CVs should therefore be flow, pressure, and temperature based avoiding cumbersome analytical measurements.

Of the 12 decision variables in Table 1, four (T_{vent}, T_{Cooler}, x_{C3}^{B1}, and x_{C9}^{D2}) are fixed at reasonable values. In mode I, there are three active constraints, x_{C9}^{D3MIN}, P_{Rxr}^{MAX}, and V_2^{MAX} along with a specified F_{C3}. In mode II, V_3^{MAX} going active sets F_{C3}. The reported values of the remaining four unconstrained decision variables (T_{Rxr}, $T_{RxrShell}$, x_{C6}^{D3}, and x_{C9}^{B3}) are then the optimum for the two modes.

In the above set of variables, compositions not related to the product quality, i.e., x_{C3}^{B1}, x_{C9}^{D2}, and x_{C9}^{B3} would usually not be available. Accordingly, we consider using appropriate temperature inferential measurements. On the purge and product columns, controlling appropriate sensitive stripping tray temperatures, T_{Col1}^{S} (7th tray; top-down numbering) and T_{Col3}^{S} (17th tray), respectively, would regulate the light key leakage down the bottoms. This would indirectly maintain x_{C3}^{B1} and x_{C9}^{B3} within a small band. The control tray locations are obtained simply as corresponding to the tray with largest tray-to-tray temperature change in the stripping section. On the recycle column, maintaining the reflux (L_2) in ratio with the column feed (B_1) would regulate the distillate cumene leakage (x_{C9}^{D2}). The product DIPB impurity mol fraction (x_{C12}^{D3}) and benzene impurity mol fraction (x_{C6}^{D3}) measurements would usually be available in an industrial setting. For on-aim product cumene mole fraction ($x_{C9}^{D3} = x_{C9}^{D3MIN} = 99.9\%$), $x_{C6}^{D3} + x_{C12}^{D3} = 0.1\%$ so that only one of the impurity mole fractions is independent. We take x_{C6}^{D3} to be independent with $x_{C12}^{D3} = 0.1\% - x_{C6}^{D3}$.

The revised practical CVs corresponding to the 12 steady state DOFs are tabulated in Table 2 along with their regulatory and economic significance. The CVs are the active constraints (or specifications) and four unconstrained CVs, T_{Rxr}, $T_{RxrShell}$, x_{C6}^{D3} and T_{Col3}^{S}. Of the unconstrained CVs, the optimum reactor inlet temperature (T_{Rxr}) and reactor coolant temperature ($T_{RxrShell}$) are nearly the same for modes I and II (see Table 1). Holding these two variables constant would likely be near optimal across the wide throughput range. For the remaining two CVs, since economic losses per unit deviation away from the optimum values are usually the highest at maximum throughput, we consider implementing the mode II optimum value at the lower throughputs. This gives a very simple constant setpoint policy across the entire throughput range. To quantify the economic loss entailed, Table 3 compares the variation with throughput in the optimum operating profit and the operating profit using the constant mode II setpoints for the above four CVs. The constant setpoint operating policy provides near optimal steady operation with the maximum profit loss being <0.21%. These four CVs may thus be deemed as SOVs that provide near optimum steady operation across the entire throughput range.

Table 2. Revised Practical CVs

SNo	CV	remarks on regulatory/economic significance
1	F_{C3}	determines process throughput.
		maximum throughput limited by V_3^{MAX}
2	F_{C6Tot}	increasing F_{C6Tot} improves selectivity
		maximum F_{C6Tot} limited by V_2^{MAX}
3	T_{Rxr}	affects reactor conversion and selectivity
		stabilizes reaction heat recycle through FEHE
4	$T_{RxrShell}$	affects reactor conversion and selectivity
		stabilizes reaction heat removal
5	P_{Rxr}	operate at P_{Rxr}^{MAX} for maximum reactor conversion
		stabilizes gas inventory in reaction section
6	x_{C6}^{D3}	determines benzene impurity level in product
		fixed by benzene dropping down the recycle column
7	x_{C12}^{D3}	determines DIPB impurity level in product
8	T_{Col3}^{S}	regulates precious cumene lost with the DIPB byproduct
9	T_{cooler}	ensures heat removal and condensation of hot reactor effluent
10	T_{vent}^{D1}	determines loss of precious benzene in the fuel gas
		should be as low as possible to minimize benzene loss
		fixed by cooling water temperature
11	T_{Col1}^{S}	regulates C_3 leakage down the purge column
12	L_2/B_1	regulates C_9 leakage in the benzene recycle stream

Table 3. Comparison of Optimum Operating Profit (J_{opt}) and Achieved Operating Profit Using Self-optimizing Control Policy (J_{SOC}) at Various Throughputs

throughput F_{C3}(kmol/h)	101.93	130	155	169.96_{Max}
optimum J_{opt} ($/h)	3802.2	4607.7	5382.7	5879.0
self-optimizing J_{SOC} ($/h)	3794.1	4597.9	5371.9	5879.0
% loss	0.21	0.21	0.20	0

ECONOMIC PLANTWIDE CONTROL STRUCTURE DESIGN

Design Procedure. The economic plantwide control structure synthesis procedure of Jagtap et al.[14] is as follows. The active constraint regions and (near) optimal steady operating policy are first obtained (step 0). In line with the "top-down" approach, pairings for the tightest possible control of economic CVs at maximum throughput, which is the most constrained operating point and therefore the most difficult to stabilize, are selected first (step 1). The economic CVs include hard equipment capacity constraints that are usually not active at the base-case (mode I) throughput. Since none of the valves are paired at this stage, the greatest flexibility in the choice of the pairings gets exploited for implementing pairings for the tightest possible control of the economic CVs. Tightest possible control of the hard equipment capacity constraints ensures the back-off from the hard limits and the consequent economic loss is the least possible. Also, loops for tight control of soft active constraints such as product quality, safety, and environmental regulation control objectives get paired in this step.

With the loops for tight control of economic CVs in place, the remaining control valves are paired for inventory (material/energy balance) control (step 2). These loops are necessary for stabilization of the individual unit operations but have only a small or negligible impact on the process steady state and hence the steady state profit. For example, pure surge levels do not have any effect on the process steady state (and therefore steady state profit). Since valves are already paired for economic CV control in step 1, the limited choice of available valves may necessitate

dx.doi.org/10.1021/ie301386h | Ind. Eng. Chem. Res. XXXX, XXX, XXX−XXX

nonlocal MVs for some of the inventory loops, i.e. long inventory loops.

The loop pairings for controlling all the inventories gives a consistent control structure for maximum throughput operation. The next step (step 3) adapts this structure for operation at lower throughputs with fewer active constraints. One of the inactive constraints gets used as the throughput manipulator, and the other inactive constraints take up additional SOV control for ensuring near-optimum operation at lower throughputs.

The long inventory loops in step 2 can sometimes result in inventory control fragility (e.g., a surge tank level hitting the high/low level alarm limit for a small flow disturbance). Should that be the case, the pairings are appropriately revised to eliminate the fragile inventory loops (step 4). Should the inventory control with the long loops be acceptable, the application of step 4 is not necessary.

We highlight that the above procedure differs fundamentally from the plantwide control design procedure of Luyben et al.[6] as well as the systematic procedure of Skogestad.[8] In both approaches, process operation around the design steady state, where no hard equipment capacity constraints are active, is considered first. While the former relies on engineering heuristics to decide the control objectives, the latter uses steady state economic optimization to choose CVs that give near optimal operation at constant setpoints. Crucial decisions such as the choice of the throughput manipulator as well as how hard equipment capacity constraints will be handled on increasing throughput (e.g., using override controllers) are only considered later after pairings have been decided for mode I (unconstrained design throughput) operation. In contrast to these extant approaches, in our approach, the regulatory implications of the additional equipment capacity constraints must necessarily be accounted for to ensure consistency of the control system at maximum throughput operation. This workable control system for the most constrained and hence difficult to stabilize operating point is then easily adapted for lower throughputs. The "top-down" higher prioritization to the mode II economic CVs (including hard equipment capacity constraints) ensures the tightest possible control of economic CVs. Its economic benefit is then significant as the most constrained operating point is usually where the economic penalty per unit back-off from a hard active constraint limit is the highest.

It is worth pointing out that Skogestad[8] uses a "bottom-up" loop pairing philosophy, where first the material/energy balance (inventory) control loops are first implemented followed by supervisory economic CV control loops. Some of the economic loops may then be "long" with consequent lose control and economic loss. The pairing philosophy in Luyben's approach is "top-down". Their procedure however ignores hard equipment capacity constraints and the need for a back-off from these hard limits naturally leads to higher economic loss. Our approach may thus be summarized as the application of a "top-down" pairing philosophy to the most constrained maximum throughput operating point for significant economic benefit.

Step 0: Obtain Active Constraint Regions and Optimal Operating Policy. The active constraint regions and optimal operating policy (step 0) have already been obtained in the previous section. For the throughput range considered, there is only one active constraint region corresponding to V_3^{MAX} going active at maximum throughput. We now design the economic plantwide control structure applying steps 1−3.

Step 1: Pair Loops for Tight Economic CV Control. The hard active constraints at maximum throughput are V_2^{MAX} and V_3^{MAX}. These are economically important as a back-off from V_2^{MAX} reduces the benzene recycle rate with loss in reactor selectivity while a back-off in V_3^{MAX} causes a loss in throughput. To minimize the back-off, V_2 and V_3 are controlled tightly using the respective reboiler duties (Q_{Reb2} and Q_{Reb3}) (first and second loops). P_{Rxr}^{MAX}, another economically important active constraint due to its impact on the reactor conversion, is considered a soft constraint. The reactor pressure is controlled tightly around its maximum value ($P_{Rxr}^{SP} = P_{Rxr}^{MAX}$) by manipulating the pressure regulatory valve (PRV) between the reaction and separation sections (third loop). The pairing would provide tight reactor pressure control.

Economic operation requires tight control of the product impurity levels for on-aim product purity of x_{C9}^{D3MIN}, a soft active constraint. For maintaining x_{C9}^{D3}, the two principal impurities in the product, C_{12} and C_6, must be maintained. Control of x_{C12}^{D3} is accomplished by adjusting the product column reflux to feed ratio (L_3/B_2) (fourth loop). The ratio scheme helps mitigate the variability in $x_{C12}{}^{D3}$ due to the feedforward action of the ratio controller to column feed flow disturbances. With regard to the C_6 impurity in the product, note that all the C_6 that leaks down the recycle column ends up in the product. Tight regulation of the C_6 leakage down the recycle column can be achieved by maintaining a sensitive stripping tray temperature (T_{Col2}^{S}). The temperature of the 11th tray (top-down numbering) is controlled as it corresponds to the location with the largest stripping section tray-to-tray temperature change. Since V_2^{MAX} constraint is active, we may use the feed to the recycle column (B_1) or the recycle column reflux rate (L_2) as the MV. The former would be effective for a mostly liquid feed and the latter must be used for a mostly vapor feed. For the specific choice of the design pressures of the purge and recycle columns, the B_1 vapor fraction is ∼25% so that the $T_{Col2}^{S}-B_1$ pairing is selected. The T_{Col2}^{SSP} is adjusted by a x_{C6}^{D3} composition controller (fifth loop). The product impurity mol fraction setpoints are chosen as x_{C6}^{D3SP} = 0.05% (mode II optimum value) and x_{C12}^{D3SP} = 0.1% − x_{C6}^{D3SP} = 0.05%. These setpoints are held constant at lower throughputs for near optimal operation.

Economic operation requires the cumene (expensive product) leakage down the product column bottoms to be small. This is achieved by maintaining a product column stripping tray temperature (T_{Col3}^{S}). Since V_3^{MAX} is active and the column feed (B_2) is mostly liquid, the $T_{Col3}^{S}-B_2$ pairing is chosen (sixth loop). Also, to keep the benzene loss in the fuel gas stream as small as possible, the purge column condenser temperature (T_{vent}) is maintained at the lowest possible value of 32 °C (limited by cooling water) by manipulating the purge column condenser duty (Q_{Cnd1}) (seventh loop).

Lastly, maintaining a high reactor conversion for a small propylene loss in the fuel gas stream as well as a high reactor selectivity for small loss of precious raw materials as DIPB byproduct are economically important objectives. Holding the reactor inlet temperature constant at 322 °C and the reactor shell side coolant temperature at 367 °C ensure that the reactor conversion and selectivity are maintained at high values across the entire throughput range. T_{Rxr} is controlled tightly by manipulating the furnace duty (Q_{fur}) for tight control (eighth loop). $T_{RxrShell}$ = 367 °C is a direct input (MV) to the process as the constant coolant temperature model is used in the simulations (ninth loop). In practice, since the reactor temperature is high, a proprietary heating oil such as Dowtherm would be used as the coolant with high pressure steam being generated in a downstream Dowtherm heated boiler. $T_{RxrShell}$

dx.doi.org/10.1021/ie301386h | Ind. Eng. Chem. Res. XXXX, XXX, XXX−XXX

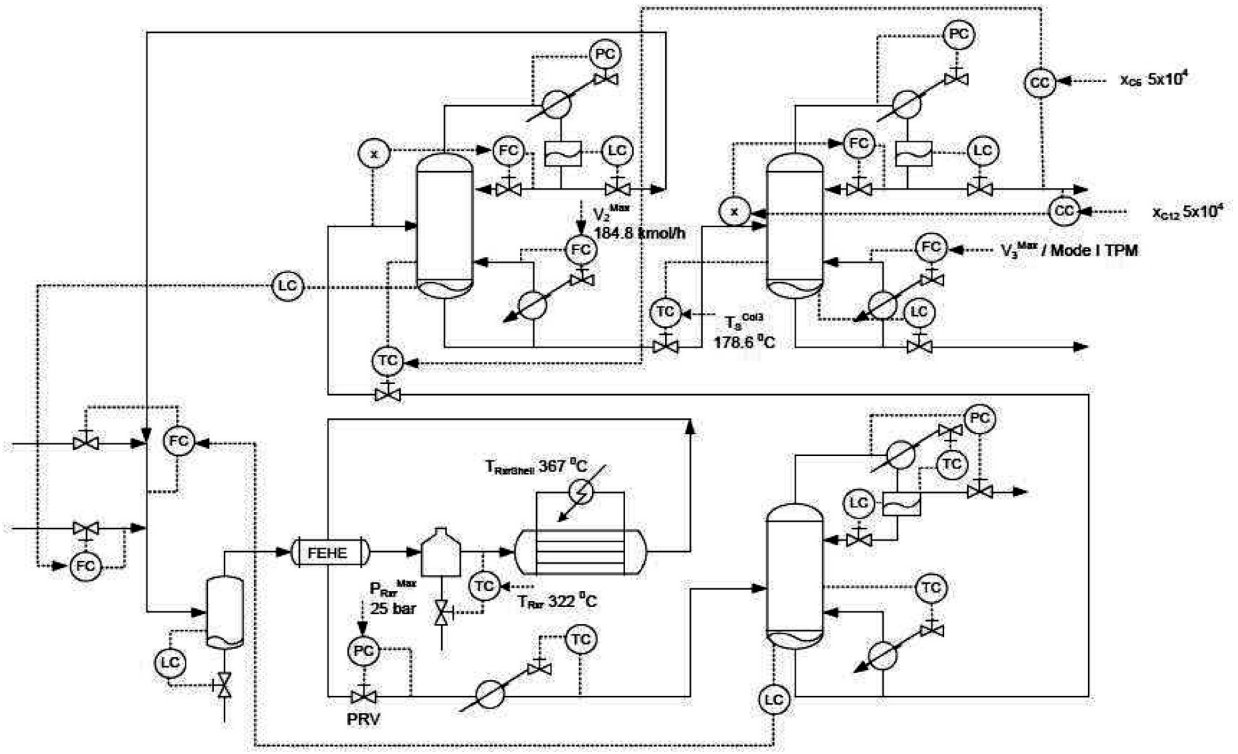

Figure 3. Economic plantwide control structure (CS1)

then is controlled by adjusting the boiler pressure setpoint with the boiler pressure being controlled by the exit steam flow.

Step 2: Design Inventory/Regulatory Control Loops. We now pair loops for inventory regulation, inventory being interpreted in its most comprehensive sense to include total material, phase, components, and energy. Of the 12 steady state DOFs, 9 loops have already been implemented in step 1. This leaves three additional loops that need to be configured plus loops for regulating the reflux drum and bottom sump levels on the three columns along with the column pressures and the feed vaporizer level.

The three additional loops correspond to holding L_2/B_1, T^S_{Col1}, and T_{Cooler} at their design values. The purge column stripping tray temperature (T^S_{Col1}) is controlled using its boilup (V_1) to regulate the C_3 leakage down the bottoms (10th loop). Maintaining L_2/B_1 using a feed to reflux ratio controller (11th loop) regulates the C_9 leakage in the benzene recycle stream. The reactor effluent condensate temperature (T_{Cooler}) is controlled by manipulating the effluent cooler duty (Q_{Cooler}) (12th loop). This ensures proper regulation of the gas/vapor inventory in the reaction section in conjunction with the P_{Rxr} control loop.

The recycle and product column pressures (P_{Cnd1} and P_{Cnd2}) are regulated by the respective condenser duty valves, Q_{Cnd2} and Q_{Cnd2} (13th and 14th loops). The purge column pressure (P_{Col1}) is regulated by the vent rate, D_1 (15th loop). Its reflux drum level (LVL_{RD1}) is regulated by manipulating the reflux (L_1) (16th loop). The feed vaporizer level (LVL_{Vap}) is regulated by the vaporizer duty (Q_{Vap}) (17th loop). The recycle column and product column reflux drum levels (LVL_{RD2} and LVL_{RD3}) are regulated using the respective distillate rates (D_2 and D_3) (18th and 19th loops). The product column bottom sump level (LVL_{Bot3}) is regulated using its bottoms rate (B_3) (20th loop). With these pairings, no close-by valves are left for regulating the purge column and recycle column bottom sump levels (LVL_{Bot1} and LVL_{Bot2}). The only option is to manipulate the two fresh feeds, F_{C3} and F_{C6}. C_3 is the limiting reactant with near complete single-pass conversion so that F_{C3} determines the cumene and DIPB production in the reactor. Since the cumene and DIPB accumulate at the bottom of the recycle column, the $LVL_{Bot2}-F_{C3}$ pairing is implemented for recycle column sump level control with the $LVL_{Bot1}-F_{C6}$ pairing being implemented for purge column sump level control (21st and 22nd loops).

Step 3: Additional SOV Control at Low Throughputs and Throughput Manipulation Strategy. In this example, there is only one active constraint region corresponding to V_3^{MAX} going active at maximum throughput with the other constraints/specifications being fixed at their mode II values at lower throughputs. The throughput may be reduced by reducing V_3 below V_3^{MAX}. V_3^{SP} is then the throughput manipulator (TPM) adjusted to operate the plant at the desired throughput below maximum. There are no additional SOVs whose control needs to be taken up at lower throughputs as no additional constraints become inactive at lower throughputs.

The economic plantwide control structure, labeled CS1, obtained by the application of steps 1−3 is shown in Figure 3. CS1 has been designed for the tightest possible control of the economic CVs using close by MVs. Since control valves get used up in these loops, in the inventory control system, the MVs of the bottom sump level loops for the purge and recycle columns are not local to the respective units but away at the fresh feeds and thus very unconventional. Even so, acceptable level regulation is expected as the lag associated with the reaction section is small with the material essentially flowing through a long pipe with small vaporizer and the reactor effluent cooler lags. The acceptable level regulation and overall process stabilization was confirmed from rigorous dynamic simulations so that application of step 4 (pairing revision to eliminate fragile inventory loops) is not necessary. With the unconventional long level loops, the

dx.doi.org/10.1021/ie301386h | Ind. Eng. Chem. Res. XXXX, XXX, XXX−XXX

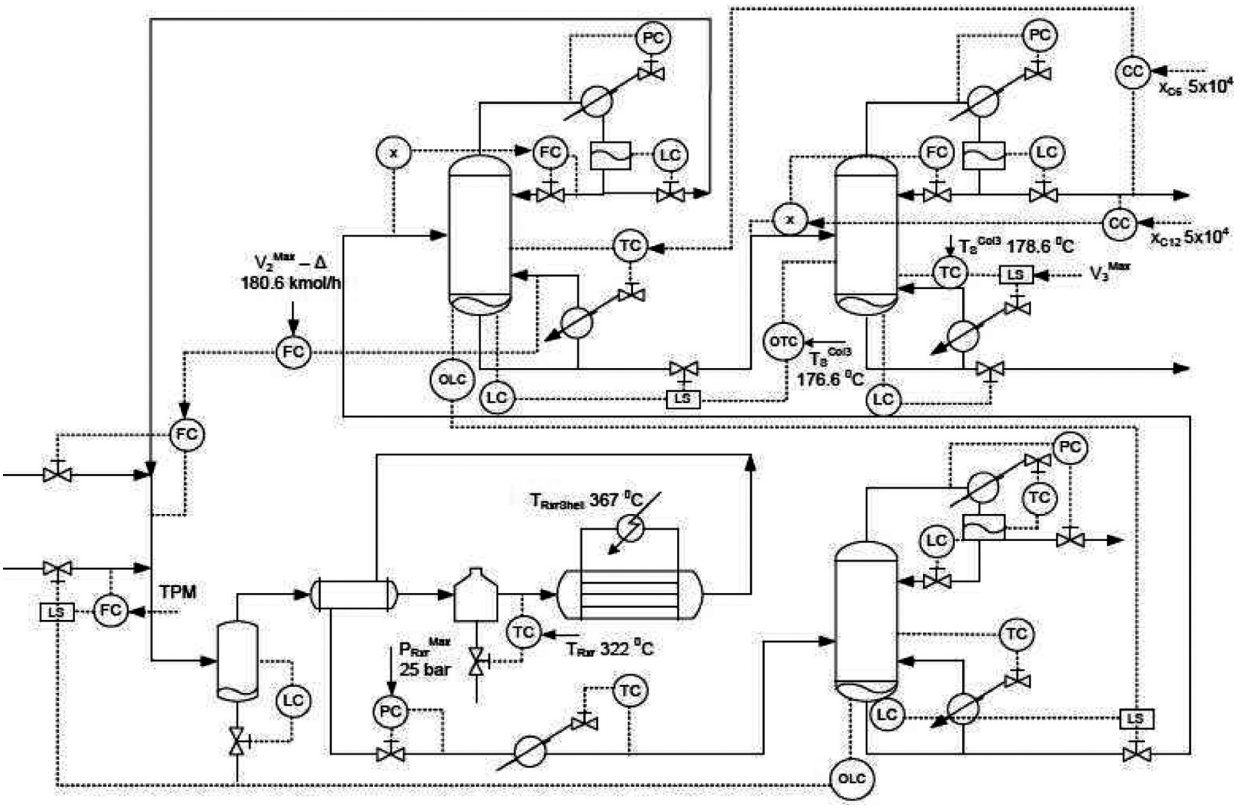

Figure 4. Conventional plantwide control structure, CS2, with overrides

control structure attempts tight control of the economic CVs with loose level control. In other words, the structure attempts tight control of the economic CVs by transforming the transients to the surge levels that have no steady state economic impact.

CONVENTIONAL PLANTWIDE CONTROL STRUCTURE

The conventional plantwide control structure, CS2, shown in Figure 4, is synthesized as follows. The TPM is at the C_3 (limiting reactant) feed (first loop). Conventional local pairings for proper inventory (material/energy) regulation of the various units downstream of the TPM are first put in place. In the reaction section, LVL_{Vap} is controlled by Q_{Vap}, T_{Rxr} is controlled by Q_{Fur}, $T_{RxrShell}$ is set at its near optimum value, P_{Rxr} is controlled at P_{Rxr}^{MAX} by the PRV, and the partially condensed reactant effluent temperature (T_{Cooler}) is maintained by its cooling duty, Q_{Cooler} (second−sixth loops). Next, conventional level and pressure loops in the distillation train are put in place. The recycle and product column pressures are controlled by the respective condenser duties while the purge column pressure is controlled by the vapor vent (seventh−ninth loops). On the purge column, the reflux drum and sump levels are controlled using the reflux and bottoms, respectively, while the overhead condenser temperature is maintained by the condenser duty (10th−12th loops). Similarly, on the recycle and product columns, the reflux drum and sump levels are regulated using the corresponding distillate and bottoms streams, respectively (13th−16th loops).

With material and energy balance loops on the individual units in place, we now put in place component inventory control loops. To regulate the C_3 leakage down the bottoms of the purge column, T_{Col1}^{S} is maintained by V_1 (17th loop). On the recycle column, L_2 is maintained in ratio with the column feed (B_1) to regulate the overhead cumene leakage (18th loop). To regulate the benzene leakage down the bottoms, T_{Col2}^{S} is maintained by V_2 with T_{Col2}^{SSP} being adjusted to maintain the product benzene impurity x_{C6}^{D3} (19th loop). On the product column, the reflux (L_3) is maintained in ratio with the feed (B_2) and L_3/B_2^{SP} is adjusted to maintain the product impurity x_{C12}^{D3} (20th loop). To regulate the cumene leakage down the product column bottoms, T_{Col3}^{S} is maintained by adjusting V_3 (21st loop). Finally, to mitigate snowballing in the recycle loop, the total (fresh + recycle) benzene, F_{C6Tot}, is maintained by adjusting the fresh benzene, F_{C6} (22nd loop). This completes the basic regulatory control structure for safe, stable and on-aim product quality process operation around the base−base (mode I) steady state.

We now adapt this basic control structure for handling the hard equipment capacity constraints. Since optimal operation requires running the process at V_2^{MAX} at all throughputs, a supervisory controller is installed that adjusts the total benzene setpoint (F_{C6Tot}^{SP}) to maintain V_2 at its near maximum setpoint. Since V_2^{MAX} is a hard constraint corresponding to the initiation of recycle column flooding and since control of the stripping tray temperature (T_{Col2}^{S}) must never be lost to ensure the product benzene impurity level is always regulated, some back-off from the V_2^{MAX} limit would be needed to ensure the hard constraint is not violated during worst case transients.

The other hard constraint that must be handled is V_3^{MAX}, the bottleneck constraint, which goes active as throughput is increased toward maximum. When V_3^{MAX} goes active, product column temperature control (T_{Col3}^{S}) is lost implying loss of precious cumene down the bottoms with a severe economic penalty. To avoid the same, an override control system is put in place that alters the material balance control structure all the way up to the C_3 feed to ensure that column temperature control is not lost when V_3^{MAX} goes active, as in Figure 4.

dx.doi.org/10.1021/ie301386h | Ind. Eng. Chem. Res. XXXX, XXX, XXX−XXX

Table 4. Prioritization of Control Objectives and Pairing Sequence Followed in Economic (CS1) and Conventional (CS2) Plantwide Control Structure Synthesis

CS1			CS2		
economic loops	constraints	$V_2^{MAX}-Q_{Reb2}$	TPM		F_{C3}
		$V_3^{MAX}-Q_{Reb3}$ [a]			
		P_{Rxr}^{MAX}–PRV	unit material/energy balance loops	reaction section	$LVL_{Vap}-Q_{Vap}$
					$T_{Rxr}-Q_{Fur}$
	product quality	$x_{C12}^{D3}-L_3/B_2-L_3$			$T_{RxrShell}$
		$x_{C6}^{D3}-T_{Col2}^{S}-B_1$			P_{Rxr}–PRV
					$T_{Cooler}-Q_{Cooler}$
	material loss	$T_{Col3}^{S}-B_2$			
		$T_{vent}-Q_{Cnd1}$		separation section	$P_{Col1}-D_1$
					$P_{Col2}-Q_{Cnd1}$
	conversion selectivity	$T_{Rxr}-Q_{Fur}$			$P_{Col3}-Q_{Cnd3}$
		$T_{RxrShell}$			$LVL_{RD1}-L_1$
					$LVL_{Bot1}-B_1$
other inventory loops	minor steady state effect	$T_{Col1}^{S}-V_1$			$T_{Vent}-Q_{Cnd1}$
		L_2/B_1-L_2			$LVL_{RD2}-D_2$
		$T_{Cooler}-Q_{Cooler}$			$LVL_{Bot2}-B_2$
		$P_{Col1}-D_1$			$LVL_{RD3}-D_3$
		$P_{Col2}-Q_{Cnd2}$			$LVL_{Bot3}-B_3$
		$P_{Col3}-Q_{Cnd3}$			
			component balance loops	separation section	L_2/B_1-L_2
	no steady state effect	$LVL_{RD1}-L_1$			$T_{Col1}^{S}-V_1$
		$LVL_{Vap}-Q_{Vap}$			$x_{C6}^{D3}-T_{Col2}^{S}-V_2$ [b]
		$LVL_{RD2}-D_2$			$x_{C9}^{D3}-L_3B_2-L_3$
		$LVL_{RD3}-D_3$			$T_{Col3}^{S}-V_3$ [c]
		$LVL_{Bot3}-B_3$			
		$LVL_{Bot1}-F_{C6}$	overall benzene balance		F_{C6Tot} [b] $-F_{C6}$
		$LVL_{Bot2}-F_{C3}$			

[a] V_3^{SP} used as TPM for below maximum throughputs. [b] F_{C6Tot}^{SP} manipulated for near V_2^{MAX} operation at all throughputs. [c] Material balance structure altering overrides necessary at V_3^{MAX}.

The override scheme works as follows. The override temperature controller on the product column is direct acting and has its setpoint slightly below the $T_{Col3}^{S}-V_3$ loop setpoint. Thus when V_3^{MAX} is inactive, its output is high and B_2 controls the recycle column sump level. When V_3^{MAX} goes active, product column temperature decreases below the override temperature controller setpoint and its output ultimately decreases below the LVL_{Bot2} controller output with the low select passing the manipulation of B_2 from the LVL_{Bot2} controller to the override temperature controller. Once this occurs, LVL_{Bot2} control is lost and it rises. The second LVL_{Bot2} override controller then takes over manipulation of B_1 via the low select in a manner similar to the product column temperature override scheme. This causes LVL_{Bot1} control to be lost and, the second LVL_{Bot1} override controller ultimately takes over F_{C3} manipulation. The override scheme thus works to cut down on the fresh propylene feed on V_3^{MAX} going active.

This completes the synthesis of the plantwide control structures using our "top-down" approach (CS1) as well as the "bottom-up" conventional approach (CS2). Table 4 summarizes the order in which the pairings have chosen in the two approaches. Note that even as many of the loop pairings are the same in both the structures, the prioritization that leads to these pairings is very different. The main difference in CS1 over the conventional structure is in the location of the TPM at the last constraint to go active (V_3^{MAX}) and the consequent upstream inventory loop pairings in the reverse direction of process flow. It is also worth mentioning that the CVs in both the structures are the same and yet the control structures are different. This is a direct consequence of the higher prioritization of the economic control objectives, including all active constraints, in CS1.

DYNAMIC SIMULATION, RESULTS, AND DISCUSSION

Rigorous dynamic simulations are performed in Unisim to evaluate and compare the performance of the synthesized economic plantwide control structure, CS1, with the conventional plantwide control structure, CS2 (including supervisory controller and overrides).

Controller Tuning Procedure. A consistent procedure is used to tune the various controllers. All flow and pressure controllers are proportional and integral (PI) and tuned for a fast and snappy response. All conventional level controllers with local unit specific pairings are P only and use a gain of 2 to smooth out flow transients. The temperature controllers are PI with a 45 s sensor lag.[17] The Unisim autotuner is used to obtain a reasonable value of the reset time and controller gain (K_C). The K_C is then adjusted for a fast but not-too-oscillatory servo response. All composition controllers use a sensor dead-time and sampling time of 5 min.[17] The autotuner does not provide reasonable initial tuning parameters so that the open loop response is first obtained and the reset time set to 2/3rd open loop response completion time and K_C set to the inverse of the process gain. These tunings work well for the two product impurity controllers in both CS1 and CS2.

In CS1, the unconventional nonlocal LVL_{Bot1} and LVL_{Bot2} controllers are P only and are tuned initially by hit and trial to stabilize the process. The temperature and composition loops are

dx.doi.org/10.1021/ie301386h | Ind. Eng. Chem. Res. XXXX, XXX, XXX–XXX

Table 5. CS1 and CS2 Controller Parameters[a]

CV attributes			CS1			CS2		
CV	set point	sensor span	MV	K_C	τ_i (min)	MV	K_C	τ_i (min)
T^S_{Col1}	140 °C	115−175 °C	Q_{Reb1}	0.2	8	Q_{Reb1}	0.2	8
T^S_{Col3}	178.64 °C	150−200 °C	B_2	0.18	20	Q_{Reb3}	0.5	15
T_{rxr}	322 °C	301−360 °C	Q_{Fur}	0.3	2	Q_{Fur}	0.3	2
T_{Cooler}	100 °C	70−130 °C	Q_{Cooler}	0.4	8	Q_{Cooler}	0.4	8
x^{D3}_{C6}	0.0005	0.0001−.0015	T^S_{Col2}	0.40	40	T^S_{Col2}	0.4	40
x^{D3}_{C12}	0.0005	0.0001−.0030	L_3/B_2	0.08	30	L_3/B_2	0.08	30
V_2	184.8 kmol/h	0−250 kmol/h	Q_{Reb2}	0.5	0.3	F^{Total}_{C6}	0.4	60
T^{SOR}_{Col3}	176.64 °C	150−200 °C				B_2	0.4	20
LC^{OR}_{Col2}	45%	0−100%				B_1	4	
LC^{OR}_{Col1}	70%	0−100%				F_{C3}	0.5	

[a]All level loops use K_C = 2 unless otherwise specified. Pressure/flow controllers are tuned for tight control.

then tuned as discussed above. Finally, the nonlocal level controller tunings are further refined for a smooth overall plantwide response to the principal disturbances. In CS2, the product column override temperature controller setpoint is chosen to the highest possible value so that the override controller never goes active for the different disturbance scenarios. This gives a setpoint that is 2 °C below nominal. The LVL_{Bot1} and LVL_{Bot2} override setpoints are chosen 10% above the nominal setpoint of 50%. Also, aggressive tuning is attempted to ensure F_{C3} is cut quickly when V_3^{MAX} goes active to mitigate the loss of precious cumene down the product column bottoms during the transient. Both the override level controllers are P only. Finally, the supervisory recycle column boilup controller is tuned for a not-too-oscillatory servo response. The salient controller tuning parameters and setpoints thus obtained are reported in Table 5 for CS1 and CS2.

Plantwide Dynamic Responses. CS1 and CS2 are dynamically tested for different disturbance scenarios. First, the dynamic transition from mode I to II is simulated. The dynamic response is also obtained for a ±10% throughput step change and a ±3% step change in the feed propylene mole fraction for mode I (F_{C3} = 101.93 kmol/h) operation. For mode II, the dynamic response is obtained for the latter as well as a ±5% step bias in the F_{C3} flow sensor. For convenience, the CS2, supervisory V_2 controller setpoint is set at V_2^{MAX} even as in practice sufficient back-off would be provided to ensure the hard V_2^{MAX} constraint is never violated during worst case transients and benzene impurity control in the product cumene is never lost.

We first consider throughput transition using CS1 and CS2, from mode I (low throughput) to mode II (maximum throughput) and back. In both structures, the TPM is ramped at a rate that causes F_{C3} to change by ∼10 kmol in 15 h. This ensures that the severity of the throughput transition disturbance is comparable in both the structures. For the throughput transition in CS1, V_3^{SP}, is ramped up at a rate of 0.79 kmol/h^2 to V_3^{MAX}, held constant for 20 h and then ramped back down at the same rate. In CS2, F_{C3}^{SP} is ramped at a rate of 0.74 kmol/h^2 until 184 kmol/h (or lower if override takes over F_{C3} manipulation), held there for about 30 h to allow for the overrides to take over and stabilize, and then ramped back down to 101.93 kmol/h. As recommended by Shinskey,[18] we use external reset on the PI T^S_{Col3} override controller to ensure it takes up B_2 manipulation at the earliest once V_3^{MAX} goes active.

The CS1 and CS2 transient response of salient process variables is plotted in Figure 5. Tight product purity control as well as smooth plantwide transients are observed for both CS1 and CS2. In CS2, the major events of V_3^{MAX} going active (P_1), the propylene feed being cut by the LVL_{Bot1} override (P_2) and beginning of the F_{C3}^{SP} (TPM) ramp down (P_3) are shown. In the CS2 dynamic response, oscillations post LVL_{Bot1} override controller taking over F_{C3} manipulation are seen. Also, it takes about 5 h between V_3^{MAX} going active and F_{C3}^{SP} manipulation passing to the LVL_{Bot1} override. The transient x^{B3}_{C9} response for CS1 and CS2 also shows that once V_3^{MAX} goes active, the cumene leakage in the DIPB stream remains well-regulated in CS1 while in CS2 the leakage increases due to the lower T^S_{Col2} override setpoint.

To evaluate the dynamic performance of the two long level loops in CS1, Figure 6 compares the dynamic response of LBL_{Bot1} and LVL_{Bot2} using CS1 and CS2 for the throughput transition. As seen from the figure, in the entire transient period, LVL_{Bot1} and LVL_{Bot2} vary within a band of 15% and 24%, respectively, in CS1. The corresponding figures for CS2 are comparable at 16% and 24%, respectively. Thus even as CS1 consists of two long level loops, the level regulation is acceptable and not fragile.

To compare the structures for mode II operation, Figure 7 plots the dynamic response of important process variables to a ±5% step bias in the F_{C3} measurement for CS1 and CS2. The dynamic response for CS1 achieves tight product purity control with a settling time of about 10 h. Similarly, the CS2 transient response also completes in about 10 h. Note that since V_3^{MAX} is active, the CS2 T^S_{Col3}, LVL_{Bot2}, and LVL_{Bot1} overrides are on and the material balance control structure is oriented in the reverse direction of process flow.

To compare the structures for mode I operation, Figure 8 plots the plantwide dynamic response of important process variables to a step change in the TPM for a ±10% throughput change. In CS1, to bring about a 10% increase and decrease in F_{C3}, the V_3^{SP} must be changed by +22.1 and −21.9 kmol/h, respectively. In CS2, F_{C3} is directly set by F_{C3}^{SP} (TPM). The product purity and DIPB cumene loss control in CS2 is not as tight as in CS1 as the TPM for CS1 is located at the product column. In CS2, on the other hand, the TPM is at a process feed and the downstream product column gets subjected to a less severe transient due to filtering by the intermediate units. Overall, a smooth plantwide response is observed in both structures. The response completion time for CS1 and CS2 is slightly above and below 10 h, respectively.

Figure 9 compares the plantwide response of important process variables to a ±3% step change in the C_3 feed propane (inert) impurity in mode I operation. Both structures handle the disturbance well with the product purity being tightly controlled.

dx.doi.org/10.1021/ie301386h | Ind. Eng. Chem. Res. XXXX, XXX, XXX−XXX

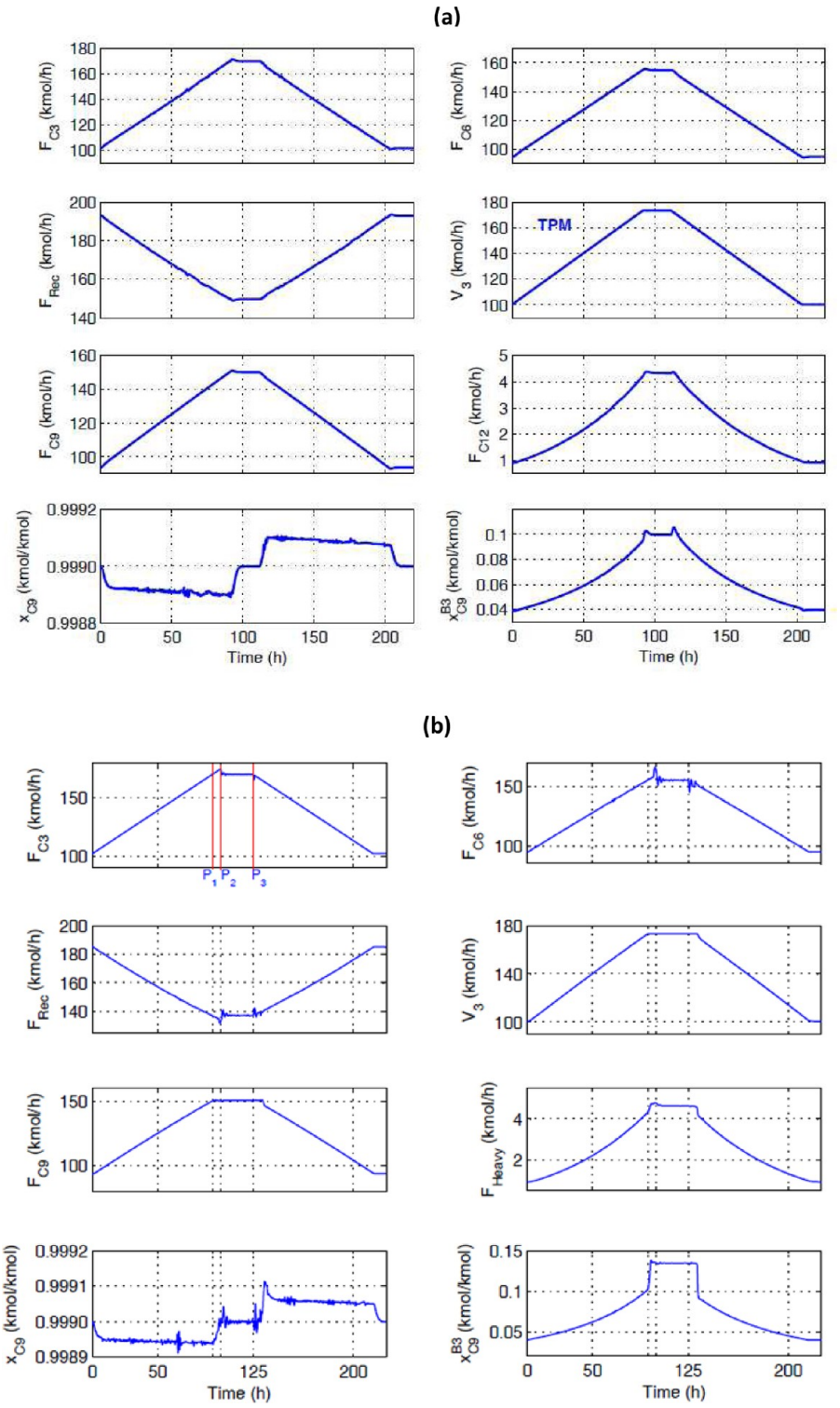

Figure 5. Transient response for throughput transition: (a) CS1; (b) CS2.

The overall plantwide response is also smooth with a response settling time of about 15 h for CS1 and about 10 h for CS2.

Quantitative Dynamic and Economic Comparison of CS1 and CS2. In this subsection, the dynamic and economic performance of CS1 and CS2 is quantitatively compared. In addition to the disturbance scenarios already considered, we consider a −5% step bias in F_{C3} measurement with the initial steady state corresponding to $(V_3 - V_3^{MAX})$ approaching 0 (Mode II). The overrides in CS2 are then 'ready to be triggered'.

To quantify the dynamic performance, the IAE values for x_{C9}^{D3} and x_{C9}^{B3} for the 10 h transient period post disturbance are reported in Table 6. From the data, it is evident that both structures provide comparable regulation of product purity and the cumene loss in the byproduct stream in mode I (V_3^{MAX} inactive) for a feed propylene composition change. For a ramped throughput change, even as the regulation of x_{C9}^{B3} is significantly poorer in CS1, it is acceptably small. As already noted, the larger x_{C9}^{B3} variability in CS1 is because the CS1 TPM (V_3^{SP}) is located at

dx.doi.org/10.1021/ie301386h | Ind. Eng. Chem. Res. XXXX, XXX, XXX−XXX

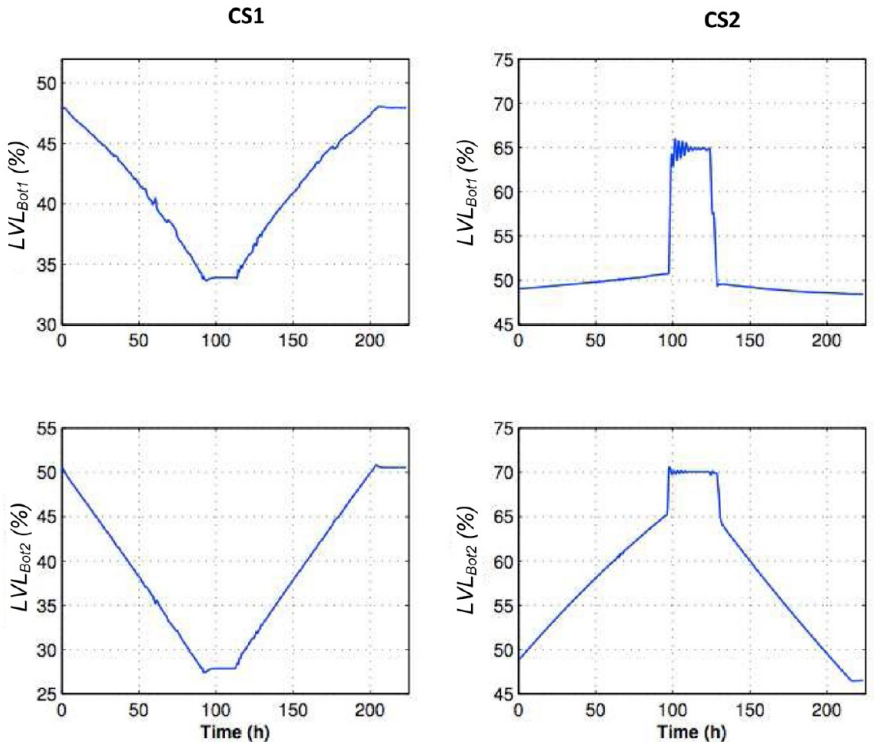

Figure 6. Comparison of LVL_{Bot1} and LVL_{Bot2} response for ramped throughput transition using CS1 (long level loops) and CS2 (conventional level loops).

the product column. The mode I throughput change data (row 1) also suggests that CS2 achieves slightly tighter product purity control. The tightness of product quality control in CS1 may be improved by maintaining the product column reflux rate in ratio with boilup, V_3 (TPM). Advanced multivariable control options may also be considered.

For mode II operation, the data (rows 3 and 4) suggests that CS1 and CS2 provide comparable dynamic regulation of x_{C9}^{D3} and x_{C9}^{B3} for process feed disturbances, namely, a 3% step change in the propylene feed composition or a 5% step bias in the F_{C3} sensor. The IAE values for x_{C9}^{B3} with the T_{Col3}^{S} override about to be triggered (last two rows) with and without external reset suggest that Shinskey's simple external reset scheme significantly improves the tightness of control by ensuring that the unselected output does not deviate too far away from the selected output due to reset windup.

To quantify the economic performance, the mode I and II steady state hourly profit is reported in Table 7. In CS2, V_2^{SP} is backed-off from V_2^{MAX} by the least amount for which the V_2^{MAX} constraint does not get violated for the worst-case disturbance scenario, which is a −5% step bias in F_{C3}, requiring the maximum back-off from V_2^{MAX}. Negligible back-off is needed in CS1 which is designed for process operation at V_2^{MAX}. Due to the back-off from V_2^{MAX} in CS2, its steady profit is slightly lower (up to >0.1% in mode II) than CS1.

To quantify economic losses during transients, Table 7 also reports the time average integral error for the 10 h transient period (T) post disturbance, defined as

$$IE_P^{Av} = \frac{\int_0^T (P_t - P_f^{SS})\, dt}{T}$$

where P_t is the instantaneous hourly profit and P_f^{SS} is the final steady state hourly profit for a disturbance. The metric is thus the time average cumulative transient profit deviation from the final steady state profit. Positive (negative) values indicate the extra hourly profit (loss) over the final steady state profit in the transient period. One would expect that any transient profit for a disturbance in one direction would be nullified by a similar transient loss for the same disturbance in the opposite direction. The IE_P^{Av} values for a given disturbance in either direction should thus be approximately the same magnitude but opposite signs. A large negative difference between the two corresponds to an unrecoverable transient economic loss. Table 7 also reports this difference

$$\Delta IE_P^{Av} = IE_P^{Av+} - IE_P^{Av-}$$

where IE_P^{Av+} and IE_P^{Av-} correspond to an increase and decrease, respectively, in the disturbance magnitude. As expected, in all but one disturbance scenario, ΔIE_P^{Av} is small for both CS1 and CS2. For a ±5% step change in the F_{C3} measurement with the CS2 overrides "ready-to-be-triggered", the ΔIE_P^{Av} is large negative implying significant unrecoverable transient losses. These losses are attributed to the excessive leakage of precious cumene in B_3 between V_3^{MAX} going active and T_{Col3}^{S} override taking over B_2 manipulation. Every extra mole of lost cumene consumes expensive reactants that cost twice the product to raw material price difference. Regardless of whether external reset is used or not on the T_{pur}^{S} override, the transient profit loss is significant at >4.5% of the steady state mode II profit. The transient loss figures with and without external reset are comparable as the oscillatory x_{C9}^{B3} response for the no external reset leads to cancellation of errors in the undershoots and overshoots.

If the CS2 overrides are switched off (e.g., by an operator), F_{C3}^{SP} must be sufficiently reduced from the maximum achievable throughput so that the V_3^{MAX} constraint does not get violated during the worst-case transient, which is a −5% step change in the F_{C3} measurement. This back-off results in a significant steady

dx.doi.org/10.1021/ie301386h | Ind. Eng. Chem. Res. XXXX, XXX, XXX−XXX

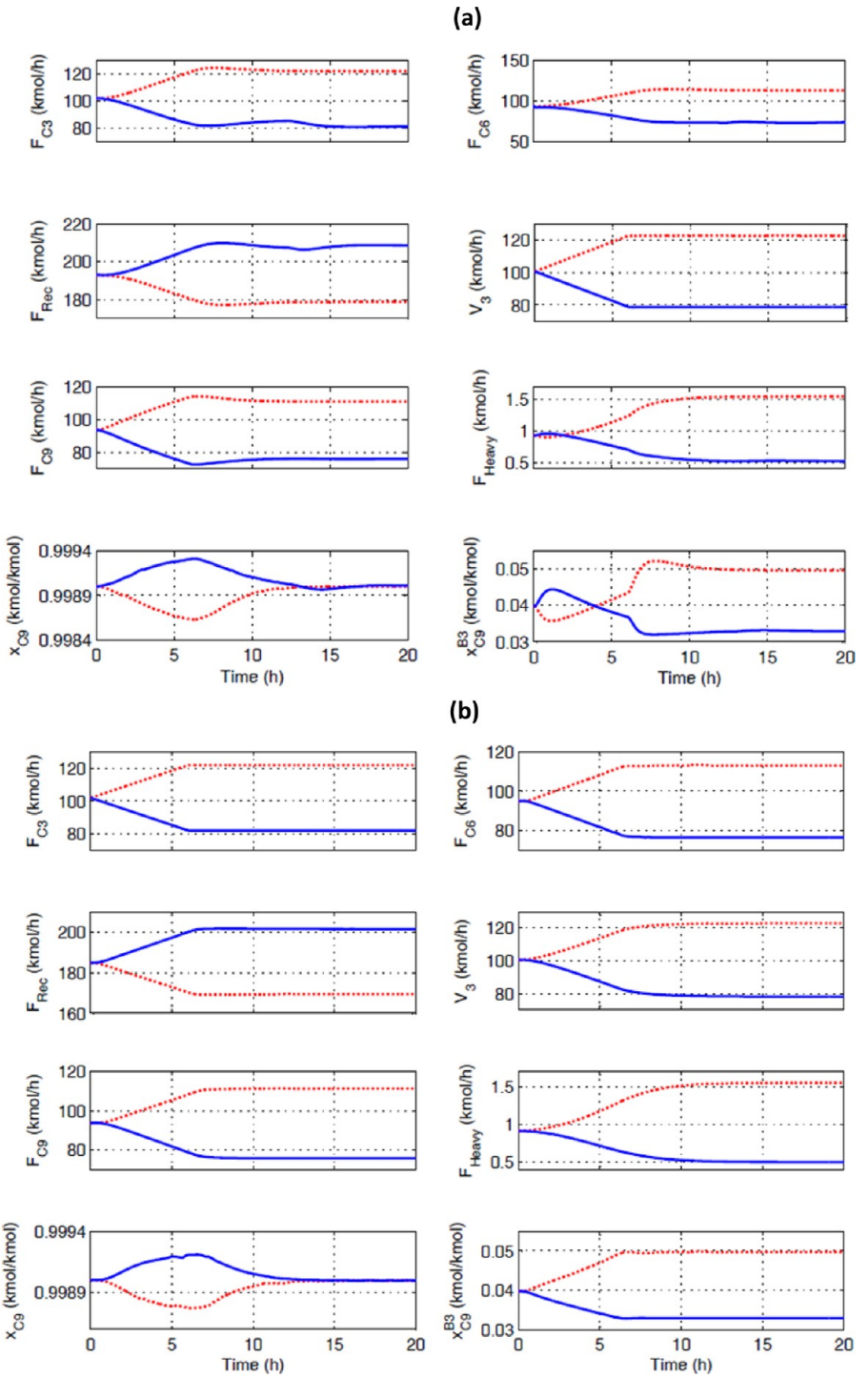

Figure 7. Mode I transient response to ±10% throughput change: (a) CS1; (b) CS2.

hourly profit loss of >4% due to lower maximum throughput. The results demonstrate that CS2 with overrides or backed-off operation results in non-negligible economic loss.

Finally, we highlight that the dynamic/economic comparison of CS1 and CS2 in Tables 6/7 is only indicative with nonrigorous tuning of the different controllers in the two structures. The economic/dynamic performance of both can be improved by tailoring the controller tunings to mitigate transients propagated toward the higher priority control objectives such as product quality/active constraints. Thus for example, the level controllers may be detuned appropriately for improved filtering of flow transients. Systematic targeted tuning of the different controllers for improved dynamic/economic performance is however a complex matter as it depends on the control structure itself, where the major disturbances enter the process as well as the transient propagation path through the plant. We hope to address this issue in future publications.

DISCUSSION

The results for the case study suggest that the economic plantwide control structure, CS1, designed for tightest possible control of the economically important hard active constraints

dx.doi.org/10.1021/ie301386h | *Ind. Eng. Chem. Res.* XXXX, XXX, XXX−XXX

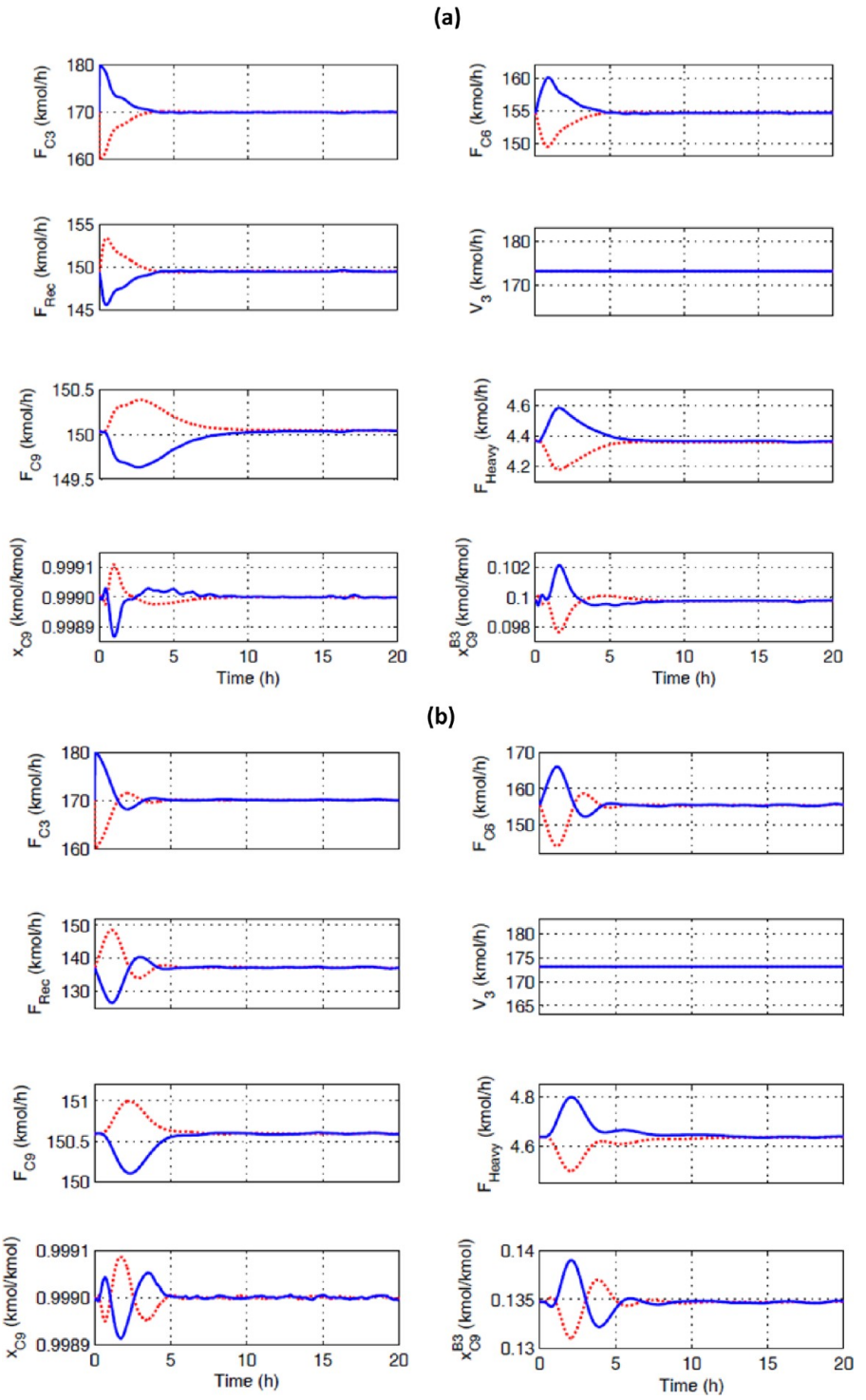

Figure 8. Maximum throughput transient response to ±5% step bias in F_{C3} sensor: (a) CS1; (b) CS2.

(V_3^{MAX} and V_2^{MAX}), achieves superior economic process operation particularly in mode II, compared to the conventional control structure, CS2. CS1 is also simpler than CS2 in that the inventory management strategy remains fixed regardless of whether the V_3^{MAX} constraint is active or not. CS2 on the other hand is more complicated requiring three additional override controllers to alter the material balance control structure all the way up to the C_3 feed, once the V_3^{MAX} constraint goes active. Proper tuning and setpoint selection of these override controllers is necessary to ensure that they get activated in the proper order without too much time elapsing between when V_3^{MAX} goes active and the overrides "take-over" control. Proper design of the override scheme can be tricky and for severe enough transients, the correct override order may get violated and large plantwide transients can occur due to the overrides taking-over and giving-up control, similar to "on−off" control. One such occurrence and operators would be inclined to turn the scheme off and resort to the more conservative backed-off process operation with a significantly more severe economic penalty.

dx.doi.org/10.1021/ie301386h | *Ind. Eng. Chem. Res.* XXXX, XXX, XXX−XXX

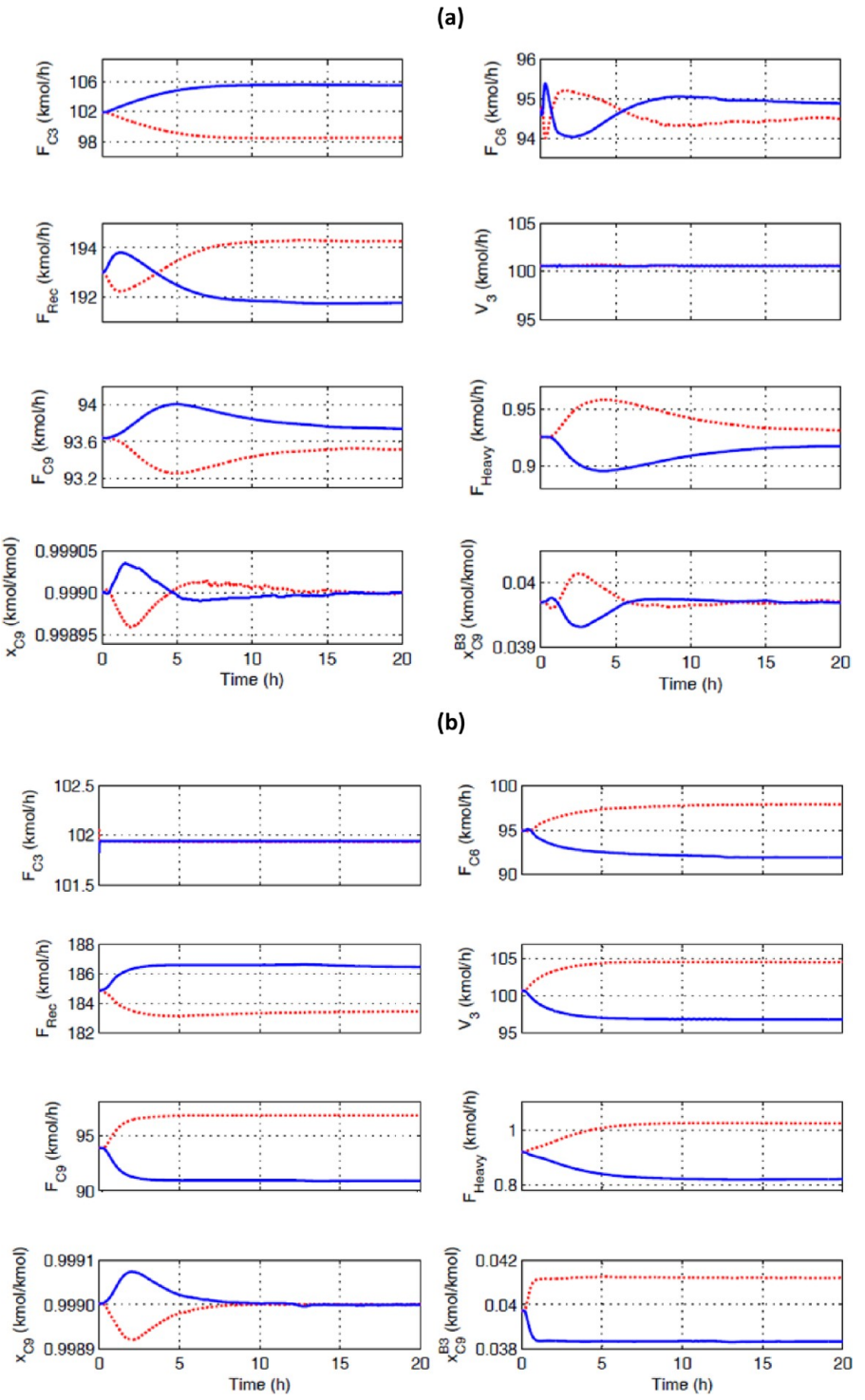

Figure 9. Mode I transient response to ±3% step in F_{C3} propylene mole fraction: (a) CS1; (b) CS2.

It is also worth noting that in our analysis, we have considered only a single disturbance to be active at a time and the hard maximum boilup constraints (V_2^{MAX} and V_3^{MAX}) to be constant. In practice, multiple disturbances are active all the time. More importantly, the hard maximum boil-up constraint limits themselves are transient, depending on the feed flow and reflux flow as well as other factors such as impurities that build-up over time inside the column. The CS2 economic performance is therefore likely to be significantly inferior to CS1 due to the need for a higher back-off in V_2^{MAX} as well as unrecoverable transient cumene loss in the DIPB stream with the override scheme switching on and off due to variability in the V_3^{MAX} limit.

The major difference between CS1 and CS2 is in the location of the TPM; V_3^{SP} for CS1 and F_{C3}^{SP} for CS2. Since V_3^{SP} is the last constraint to go active (i.e., the bottleneck constraint) and also economically important with any back-off resulting in reduced throughput, it makes sense to use it as the TPM and not for the conventional control task of tray temperature control. Typically, due to the high sensitivity of recycle flows to throughput changes (snowball effect), the bottleneck constraint is usually inside the

dx.doi.org/10.1021/ie301386h | Ind. Eng. Chem. Res. XXXX, XXX, XXX−XXX

Table 6. IAE Values for x_{C9}^{D3} and x_{C9}^{B3} for 10 h Transient Post Disturbance

disturbance scenarios			CS1		CS2	
ISS[a]	description	magnitude	x_{C9}^{D3} (10^{-3})	x_{C9}^{B3} (10^{-2})	x_{C9}^{D3} (10^{-3})	x_{C9}^{B3} (10^{-2})
mode I	throughput	+10%[b]	2.180	7.490	1.380	3.60
		−10%[b]	2.068	5.294	1.318	2.12
	C_3 feed composition	+3%	0.140	0.139	0.254	0.098
		−3%	0.118	0.125	0.263	0.073
mode II	F_{C3} sensor bias	+5%	0.171	0.341	0.187	0.808
		−5%	0.180	0.383	0.195	0.971
	C_3 feed composition	+3%	0.154	0.329	0.119	0.610
		−3%	0.152	0.305	0.114	0.524
V_3^{MAX}−δ^c	F_{C3} sensor bias[d]	+5%	0.171	0.341	0.868	1.326
		−5%	0.180	0.383	0.550	24.247
	F_{C3} sensor bias[e]	+5%	0.171	0.341	0.876	1.058
		−5%	0.180	0.383	0.370	3.602

[a]Initial steady state [b]TPM setpoint ramped over 6 h. IAE calculated over 15 h period [c]CS2 overrides are "ready to be triggered". [d]No external reset in CS2 T_{pur}^{S} override. [e]External reset in CS2 T_{pur}^{S} override.

Table 7. Steady State and Transient Profit Data for CS1 and CS2

Steady State Hourly Profit Data				
mode of operation			CS1 (10^3 \$/h)	CS2 (10^3 \$/h)
mode I			3.8082	3.8059
mode II			5.8790	5.8527
Transient Profit Data (IE_P^{Av} and ΔIE_P^{Av} Values)				
disturbance scenarios			CS1	CS2
ISS[a]	description	magnitude	IE_P^{Av} (\$/h)	ΔIE_P^{Av} (\$/h)	IE_P^{Av} (\$/h)	ΔIE_P^{Av} (\$/h)
mode I	throughput	+10%	132.76	5.91	−277.15	−2.21
		−10%	−126.84		274.94	
	C_3 feed composition	+3%	−59.46	13.47	11.45	−6.49
		−3%	72.93		−17.94	
mode II	F_{C3} sensor bias	+5%	119.08	−11.99	125.51	12.41
		−5%	−131.07		−113.10	
	C_3 feed composition	+3%	−17.46	−0.45	−22.26	1.69
		−3%	17.01		23.95	
V_3^{MAX}−δ^c	F_{C3} sensor bias[d]	+5%	119.08	−11.99	98.38	−285.22
		−5%	−131.07		−383.60	
	F_{C3} sensor bias[e]	+5%	119.08	−11.99	101.42	−262.94
		−5%	−131.07		−364.36	

[a]Initial steady state. [b]TPM setpoint ramped over 6 h. IAE calculated over 15 h period. [c]CS2 overrides are "ready to be triggered". [d]No external reset in CS2 T_{pur}^{S} override. [e]External reset in CS2 T_{pur}^{S} override.

recycle loop. The case study results support the heuristic of locating the TPM at the bottleneck constraint for economic operation.

Lastly, we highlight that the conventional practice in control structure design is to implement inventory control loops with their MVs being "local" to the specific unit containing the inventory. The basic idea is to ensure that the inventory loops are robust. This case study illustrates that it is possible to develop control structures with seemingly unworkable "long" inventory control loops that provide acceptable regulation with tight control of the economic CVs over the entire throughput range. The top-down pairing philosophy, as illustrated here should be applied to come up with such unconventional but workable economic plantwide control structures, in the knowledge that should the inventory control be fragile, the pairings can always be revised toward "local" inventory loops and "long" economic loops in lieu.

CONCLUSIONS

In conclusion, this article demonstrates through a case-study, the crucial role of economically important maximum throughput hard active constraints in determining the input−output pairings for economic plantwide control. The approach demonstrated here leads to a simple control structure with unconventional inventory loops and no overrides for process operation over the tested throughput range. Conventional control systems that do not take into consideration the active constraints on the other hand must resort to complicated overrides for constraint handling at high throughputs, with overall inferior economic performance.

Additional Information. Unisim steady state and dynamic simulation files may be obtained from the corresponding author on request.

APPENDIX

A brief at-a-glance comparison of the Luyben flowsheet[15] and the slightly modified flowsheet used here, replacing the cooled

dx.doi.org/10.1021/ie301386h | Ind. Eng. Chem. Res. XXXX, XXX, XXX−XXX

reactor effluent vapor−liquid separator (flash) tank with a small distillation column, is provided below (Table A1). The price data

Table A1. At-a-Glance Comparison of Luyben and Modified Process

variable	unit	Luyben process	modified process
fresh propylene (F_{C3})	kmol/h	101.93	101.93
fresh benzene (F_{C6})	kmol/h	98.78	95.09
total benzene (F_{C6}^{Total})	kmol/h	207	207
vent	kmol/h	9.98	6.47
product (F_{C9})	kmol/h	92.86	92.94
heavy (F_{C12})	kmol/h	1.55	1.59
total capital cost	$\$10^6$	4.11	4.28
total energy cost	$\$10^6$/y	2.23	2.37
benzene cost	$\$10^6$/y	59.36	57.09
propylene cost	$\$10^6$/y	30.63	30.63
reactor steam credit	$\$10^6$/y	0.40	0.54
fuel gas vent credit	$\$10^6$/y	1.59	0.70
heavy DIPB credit	$\$10^6$/y	0.71	0.48
product revenue	$\$10^6$/y	107.74	107.87
total operation profit[a]	**$\$10^6$/y**	**18.23**	**19.50**

[a]Total operation profit = product revenue + (steam/vent/DIPB credit) − (raw material + energy cost) − capital cost/3.

in Table 1 is used while the equipment cost correlations and reactor steam credit, vent gas fuel credit, and heavy DIPB fuel credit data are taken from Luyben.[15] The economic comparison quantitatively shows that while the equipment cost of the modified flowsheet is slightly higher, the reduced benzene loss in the vapor vent leads to reduced fresh benzene consumption. The consequent reduced fresh benzene cost gives >6% higher total operation profit for the modified flowsheet.

AUTHOR INFORMATION

Corresponding Author

*E-mail: nkaistha@iitk.ac.in. Fax: +91-512-2590104. Phone: +91-512-2597513.

Present Address

[§]Currently on one-year leave at School of Chemical and Biomedical Engineering, Nanyang Technological University, Singapore 637459.

Notes

The authors declare no competing financial interest.

ACKNOWLEDGMENTS

The corresponding author acknowledges the seminal influence of Prof. Charles F. Moore in shaping his perspective on plantwide control. Funding from Erasmus Mundus External Cooperation Window (Lot 13) and Department of Science and Technology, Government of India, is also gratefully acknowledged.

REFERENCES

(1) Luyben, W. L. Snowball effects in reactor/separator processes with recycle. *Ind. Eng. Chem. Res.* **1994**, *33* (2), 299−305.

(2) Luyben, W. L.; Tyreus, B. D.; Luyben, M. L. *Plantwide Process Control*; New York: McGraw Hill, 1999.

(3) Luyben, M. L.; Luyben, W. L. Design and control of a complex process involving two reaction steps, three distillation columns, and two recycle streams. *Ind. Eng. Chem. Res.* **1995**, *34* (11), 3885−3898.

(4) Tyreus, B. D.; Luyben, W. L. Dynamics and control of recycle systems 4. Ternary systems with one or two recycle stream. *Ind. Eng. Chem. Res.* **1993**, *32* (6), 1154−1162.

(5) Luyben, M. L.; Tyreus, B. D.; Luyben, W. L. Analysis of control structures for reaction/separation/recycle processes with second order reactions. *Ind. Eng. Chem. Res.* **1996**, *35* (3), 758−771.

(6) Luyben, M. L.; Tyreus, B. D.; Luyben, W. L. Plantwide control design procedure. *AIChE J.* **1997**, *43* (12), 3161−3174.

(7) Skogestad, S. Plantwide control: The search for the self-optimizing control structure. *J. Proc. Cont.* **2000**, *10* (5), 487−507.

(8) Skogestad, S. Control structure design for complete chemical plants. *Comput. Chem. Eng.* **2004**, *28* (1−2), 219−234.

(9) Jagtap, R.; Kaistha, N.; Skogestad, S. Plantwide control for economic optimum operation of a recycle process with side reaction. *Ind. Eng. Chem. Res.* **2011**, *50* (14), 8571−8584.

(10) Jagtap, R.; Kaistha, N. Economic plantwide control of the ethyl benzene process. *AIChE J.* **2012**, DOI: 10.1002/aic.13964.

(11) Jagtap, R.; Kaistha, N. Economic plantwide control of the C_4 isomerization process. *Ind. Eng. Chem. Res.* **2012**, DOI: 10.1021/ie3001293.

(12) Araujo, A.; Skogestad, S. Control structure design for the ammonia synthesis process. *Comput. Chem. Eng.* **2008**, *32* (12), 2920−2932.

(13) Kanodia, R.; Kaistha, N. Plantwide control for throughput maximization: A case study. *Ind. Eng. Chem. Res.* **2010**, *49* (1), 210−221.

(14) Jagtap, R.; Kaistha, N.; Skogestad, S. Economic plantwide control over a wide throughput range: A systematic design procedure. *AIChE J.* **2012**, under review.

(15) Luyben, W. L. Design and control of the cumene process. *Ind. Eng. Chem. Res.* **2010**, *49* (2), 719.

(16) Gera, V.; Kaistha, N.; Panahi, M.; Skogestad, S. Plantwide control of a cumene manufacture process. *Comput.-Aided Chem. Eng.* **2011**, *29* (8), 522−526.

(17) Luyben, M. L.; Luyben, W. L. *Essentials of Process Control*; New York: McGraw Hill, 1996.

(18) Shinskey, F. G. *Process Control Systems: Application, Design and Tuning*; New York: McGraw Hill, 1996.